New Mitigation Schemes of the Ablative Rayleigh-Taylor Instability

H. Azechi 1), H. Shiraga 1), M. Nakai 1), K. Shigemori 1), S. Fujioka 1), T. Sakaiya 1), Y. Tamari 1), K. Ohtani 1), T. Watari 1), N. Ohnishi 2), M. Murakami 1), A. Sunahara 1), H. Nagatomo 1), K. Nishihara 1), N. Miyanaga 1), and Y. Izawa 1)
1) Institute of Laser Engineering, Osaka University, Suita, Japan
2) Department of Aeronautics and Space Engineering, Tohoku University, Sendai, Japan

e-mail contact of main author: azechi@ile.osaka-u.ac.jp

Abstract. The Rayleigh-Taylor (RT) instability with material ablation through the unstable interface is the key physics that determines success or failure of inertial fusion energy (IFE) generation, as the RT instability potentially quenches ignition and burn by disintegrating the IFE target. We present two suppression schemes of the RT growth without significant degradation of the target density. The first scheme is to generate double ablation structure in high-Z doped plastic targets. In addition to the electron ablation surface, a new ablation surface is created by x-ray radiation from the high-Z ions. Contrary to the previous thought, the electron ablation surface is almost completely stabilized by extremely high flow velocity. On the other hand, the RT instability on the radiative ablation surface is significantly moderated. The second is to enhance the nonlocal nature of the electron heat transport by illuminating the target with long wavelength laser light, whereas the high ablation pressure is generated by irradiating short wavelength laser light. The significant suppression of the RT instability may increase the possibility of impact ignition which uses a high velocity fuel colliding with a preformed main fuel.

1. Introduction

In order to achieve fast ignition with laser energy of several tens kJ, much less energy than that required for central-ignition, one needs efficient heating as well as high-density compression. With respect to these requirements, recent experiments have demonstrated that about 15-30% of the laser energy is converted to the thermal energy of a compressed fuel even at a laser intensity required for ignition [1]. High-density compression of more than thousand times liquid density has, therefore, become a critical subject not only for central ignition but also for fast-ignition research. This is well above the density ever achieved [2].

The Rayleigh-Taylor (RT) instability with material ablation through the unstable interface is the key physics that determines success or failure of high-density compression, as the instability potentially disintegrates the target. Unlike the classical RT instability on the boundary between two fluids with different density, the ablative RT instability has material ablation through the unstable interface. Since the ablation removes the perturbation away from the unstable surface, the RT instability may be significantly moderated. One might use the Takabe-Bodner like formula [3, 4] for the growth rate:

$$\gamma = [kg/(1+kL)]^{1/2} - \beta k v_a , \qquad (1)$$

where k is the wave number of the perturbation, g is the gravity, L is the density scale length at the ablation surface, v_a is the fluid velocity across the unstable surface (ablation velocity hereafter), and β is a numerical coefficient determining the effectiveness of the ablation effect. Betti et al. [5] have found an analytical solution that can be approximated by Eq. (1). Kull [6], Sanz [7], and Piriz [8] also found similar growth rate analytically. Although this formula is widely adopted and there are a number of experiments to compare with [9-15], it should be emphasized that the formula itself has never been tested by experiments. Our strategy is to reach proper understanding of the ablative RT instability by measuring all necessary quantities (growth rates, gravity, wave-number of the perturbation, mass ablation rate, density profile) without invoking simulation or theories. This allows us to rigorously test

our understanding of the RT instability. Since not all data have been obtained at the same experimental condition, we give only a status report in Sec 3.

It is generally believed that the ablative reduction of the growth rate given by Eq. (1) is insufficient for IFE application. Several concepts to suppress the ablative RT instability have been proposed, including impulsive acceleration [16], control of isentrop distribution by picket pulse [17], by radiation emitted from a thin metallic overcoat layer [18], by nonlocal electrons with two-color irradiation [19], double ablation in high-Z doped target [20] and distributed dopant in a capsule [21]. Although the RT suppression has to be realized without significant degradation of the target density, to date this requirement has been tested for only two concepts [19, 20]. In Sec. 4, we present two suppression schemes of the RT growth rate. One is to generate double ablation structure in high-Z doped plastic targets. In addition to the electron ablation surface, a new ablation surface is created by x-ray radiation from the high-Z ions. Contrary to the previous thought, the electron ablation surface is almost completely stabilized by extremely high flow velocity. On the other hand, the RT instability on the radiative ablation surface is significantly moderated. The second scheme is to enhance the nonlocal nature of the electron heat transport by illuminating the target with long wavelength laser light, whereas the high ablation pressure is generated by irradiating short wavelength laser light. In both schemes, the degradation of the target density was found to be minimal.

Finally, in Sec. 5, we discuss the implication of the sufficient suppression of the RT instability. It may not only increase the compressed density but also revive an old ignition idea: A high velocity implosion can configurate a hot spark without a main fuel so as to ignite at very low laser energy.

2. Experimental Condition

The experiments has been conducted at the HIPER facility [22] which combines all twelve beams of the GEKKO-XII laser facility [23] into virtually one single beam so that a large target area is irradiated at a relatively high laser intensity. The effective focusing optics of the combined beam is *f*/3. Among the twelve beams, three frequency-doubled (laser wavelength $\lambda = 0.53$ μm) beams of partially coherent light [24] were used as a foot pulse for pre-compression of the target, while the other nine frequency-tripled ($\lambda = 0.35$ μm) beams smoothed by spectral dispersion [25] along three-direction [26] were used as a main pulse for accelerating the target uniformly. Kinoform phase plates were also implemented in front of each focusing lens to obtain uniform envelope of the laser focal pattern. As for the experiment of two-color irradiation scheme described in Sec 4.2, three 1.05-μm or 0.53-μm laser beams were simultaneously overlapped with six 0.35-μm laser beams on a target.

Polystyrene targets with a 1.06-g/cc density and a 25-μm thickness were irradiated with the laser at a normal incidence at a laser intensity of about 2×10^{12} W/cm^2 on the foot and about 1×10^{14} W/cm^2 on the main pulse. In the experiment of RT suppression by double ablation described in Sec. 4.1, we used a Br doped plastic target ($C_{50}H_{41.5}Br_{3.3}$) with a mass density of 1.35 g/cc. In any case, the foot pulse intensity was adjusted so that two shock waves launched by the foot pulse and the main pulse reach the target rear surface nearly simultaneously.

The growth of the areal-mass perturbation was observed with the face-on x-ray backlighting using a Zn target as an x-ray source. The photon energy of the backlighter emission was ~1.5 keV, when combined with Al filter and the CuI photocathode response. In most experiments, we used a 12x50-μm slit as an x-ray imager for the face-on backlighting with the height direction being parallel to the perturbation ridge. In the case of short perturbation wavelength (<12 μm), we employed moiré interferometry to convert short wavelength perturbation to much longer one so as to be observables.

The foil trajectory was also measured with a separate x-ray backlighting in side-on geometry, in which the backlighter x rays flashed the target from its edge. The backlighter target was an Al foil, producing 1.5-1.8 keV x rays. The x-ray imager for the side-on backlighting was identical to that for the face-on backlighting. The imaging slit was set so that the height direction is perpendicular to the direction of the target acceleration.

Throughout the present study, we define the time zero (t=0) at the time of the first half maximum of the main laser pulse. More specific information on the experimental setup will be given in the description of each experiment.

3. Validation of Ablative Rayleigh-Taylor Instability

There were three major difficulties to measure all physical quantities. Figure 1 summarizes the techniques we innovated to overcome the difficulties. The first is that the perturbation wavelength, at which the ablation effect becomes most pronounced, exists around or even below spatial resolution of most x-ray imaging device. The growth rate at short wavelength has been measured with moiré interferometry [27]. The growth rate has been measured up to 3-μm perturbation wavelength [15].

The second is the mass flux (mass ablation rate) across the unstable interface. The mass ablation rate was inferred from the timing of x rays emitted from a plastic target sandwiched with high-Z tracer layer. However, the x-ray emission timing may be severely influenced by hydrodynamic mixing of the tracer layer into the plastic, making the mass ablation rate measurement very inaccurate [28]. Instead, mass ablation rate may be measured from time dependent x-ray transmittance [29]. Since the ablated material is heated to ~ keV temperature and hence fully ionized, the x-ray transmittance is solely due to the residual target mass. The time derivative of the residual mass gave the mass ablation rate of 3 x 10^5 g/s cm^2 at an laser intensity of 1 x 10^{14} W/cm^2 for the laser wavelength of 0.35 μm, in good agreement with our simulation prediction by ILESTA-1D [30].

The most difficult part was the ablation density measurement. The density may be deduced from x-ray transmittance through the target from the side direction with known mass absorption coefficient and the target length along the line-of-sight. The x-ray imaging device

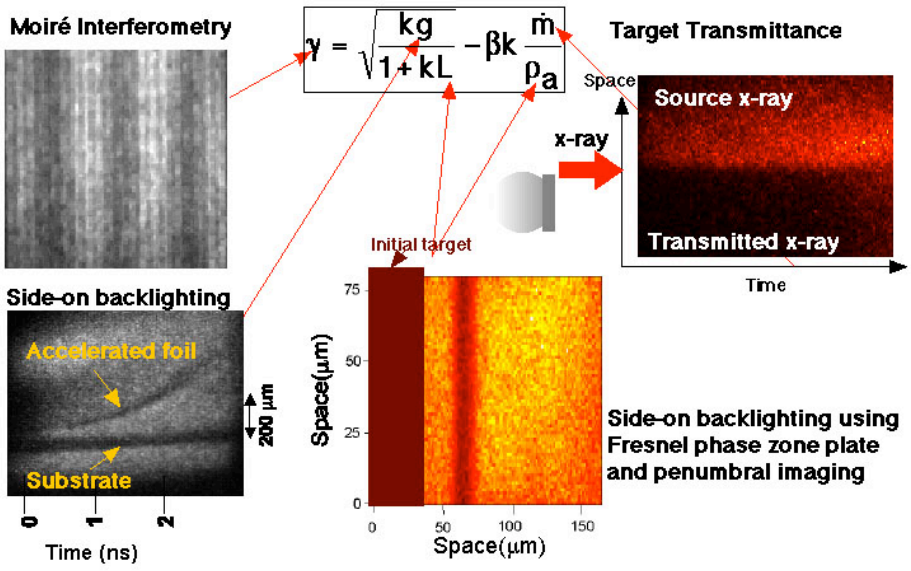

FIG. 1. Schematic view of data for full diagnostics of the ablative Rayleigh-Taylor instability. Shown are sample images of moiré interferometry for growth rates of short perturbation wavelength (left top), x-ray transmittance through a target for mass-ablation-rate (top right), side on x-ray backlighting for target trajectory (bottom left), and side-on backlighting for target density.

for this measurement must satisfy the following requirement. (1) Since the target thickness is about 10 μm after shock compression, one needs at least 3 μm resolution. (2) The x-ray photon energy of about 5 keV is needed for the x-ray to sufficiently transmit through the target. To meet these requirements we have developed two techniques: penumbral imaging [31] and Fresnel phase zone plate [32]. An example of the side-on x-ray backlighting is shown in the bottom of Fig. 1. It is observed that the target is well compressed with the thickness of about 1/3 of the initial one. The flatness of the target along the vertical direction ensures the flatness along the line-of-sight. The measured target density and inferred density scale-length were in good agreement with those predicted by ILESTA-1D, as will be described in Sec. 4.

Figure 2 shows the growth rate as a function of the perturbation wavelength with the coefficient β as a fitting parameter for 0.53- and 0.35-μm laser wavelengths. The data for a 0.53-μm laser were taken from Ref. [15]. Two curves are obtained by solving differential equation of the RT instability for the surface perturbation amplitude $a(t)$, $d^2a(t)/dt^2 = \gamma(t)^2a(t)$, using the time dependent growth rate $\gamma(t)$ given by Eq. (1) with all parameters (gravity, mass ablation rate, ablation density and density scale-length) calculated from the hydro-simulation. The calculated growth rates were then obtained by logarithmic fitting of the amplitude in the same time interval as that in the experiment. The experimental β is reasonably consistent with the theoretical prediction of $\beta = 1.7$ for plastic targets [5]. However, the experimental growth rate becomes much lower than the prediction especially for the medium wavelength region at around 20-100 μm in the 0.53-μm laser case and at around 30-100 μm in the 0.35-μm laser case.

Although further work is necessary to resolve this discrepancy, we presume that a possible mechanism to account for the stabilization is enhancement of fire-polishing (or enhanced dynamic over pressure) due to the modification of the ablative flow. In the concave region of the target, for instance, the ablative flow concentrates and blows the laser absorption region away from the target compared to that in the unperturbed case. The energy flux is reduced due to the increased distance between the ablation and the absorption region, thereby reducing the ablation pressure. The opposite is true in the convex region of the target. Moreover, focusing of laser light in the modulated flow tends to stabilize the instability.

At the short wavelength perturbations, on the contrary, the perturbation of the ablative flow is fast reduced and, therefore, the laser absorption region is unaffected. This is the situation that most theories assume.

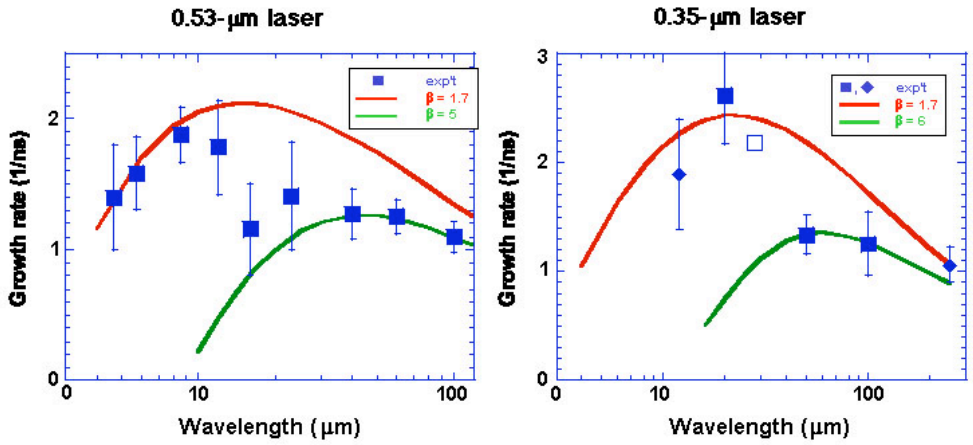

FIG. 2. Growth rates of the ablative Rayleigh-Taylor instability for 0.53-μm and 0.35-μm laser wavelengths. The left figure are from Ref. [15].

4. Suppression of the Instability.

Although the suppression at the medium perturbation wavelengths described above is favorable for IFE, further suppression of the instability is certainly needed. In this section, we will describe two intended schemes to reduce the growth rate: double ablation and two-color irradiation.

4.1. Double Ablation

When a small amount of high-Z material is doped in the ablator material, x rays are generated in the laser-irradiated high-temperature region. The generated x rays are transported to the inner and higher density region of the target and deposit their energy there, causing radiation-driven ablation, if the doped material and its density are properly chosen.

Previously, the double ablation was viewed as an undesired phenomenon because second unstable surface is introduced in addition to the original ablation surface. However, as is well known a radiation-driven ablation surface is much more stable than a generic electron-driven ablation surface because of the large ablation velocity and the long density scale-length. On the other hand the ablation velocity at this electron ablation is extremely enhanced by two factors: (1) The mass flux from the upper stream is large because of the radiation-driven ablation. (2) The electron ablation density is much less than the upper stream density.

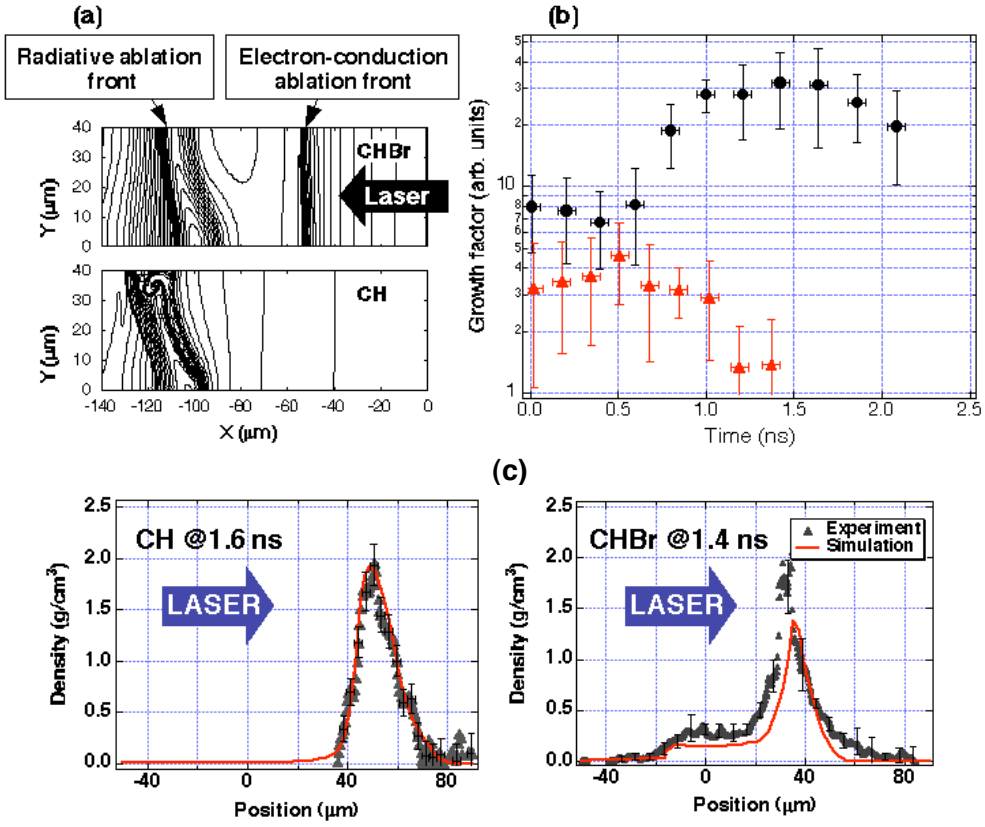

FIG. 3. Suppression of the ablative Rayleigh-Taylor (RT) instability by double ablation scheme. (a) Density contour plots showing the RT instability growth in Br doped polystyrene (CHBr) and generic polystyrene (CH) targets. (b) The observed RT growth of CH and CHBr targets with initial perturbation wavelength of 20-25 μm. (c) Density profiles of the generic CH and CHBr targets measured with the penumbral imaging. Double ablation structure is clearly seen in the CHBr target. Also shown are the profiles calculated with hydrodynamic simulation ILESTA-1D

The RT growth of the double ablation structure was investigated with a two-dimensional (2D) Eulerian radiation hydrodynamic code RAICHO [33]. The target in the simulation was a 3-atomic % Br doped polystyrene (CHBr) with a 25-μm thickness. The laser was assumed to be normally incident on the target and the laser absorption was calculated with 1D ray tracing. Wavelength and amplitude of the perturbation imposed initially on the target surface was 80 and 0.8 μm, respectively. As is expected, the 2D simulation [Fig. 3 (a)] shows that the electron-driven ablation surface is almost completely stabilized, whereas the deformation on the x-ray ablation is significantly moderated compared to that for the generic CH target. The ablation velocity of the CHBr target is three times larger than that of the CH target.

Perturbation growth in planar CHBr and CH targets was diagnosed with face-on backlighting using 1.5 keV x rays emitted from a Zn plasma. The data at relatively long perturbation wavelength of 50 μm showed that the perturbation growth on the CHBr is much lower than that of the CH target. The difference was even more pronounced at shorter perturbation wavelength of 20-25 μm, where the growth rate of the generic CH target has its maximum. The perturbation growth in CHBr was almost completely stabilized as shown in Fig. 3 (b).

Also shown in Fig. 3 (c) is the density profile of CH and CHBr targets. The double ablation structure is clearly seen in the CHBr target, in sharp contrast to the single ablation structure in the CH target. The peak density of the CHBr target is only slightly lowered and no serious disassembly was observed. A comparison was also made with the prediction by ILESTA-1D simulation. Although the agreement is quite good for the CH target, the density profile of the CHBr target disagrees with the prediction. This is probably due to the inaccurate atomic model (average atom model) used in the simulation.

4.2. Two-Color Irradiation

It has been found that in the case of relatively long laser wavelengths of 0.53 μm or longer, nonlocal electron heat transport plays a significant role to reduce the RT growth rate [9, 10, 11]. Near the critical density region of the laser light (about 1/100 of solid density), electrons are heated to high temperature (a few keV) so that the electron mean-free-path becomes a

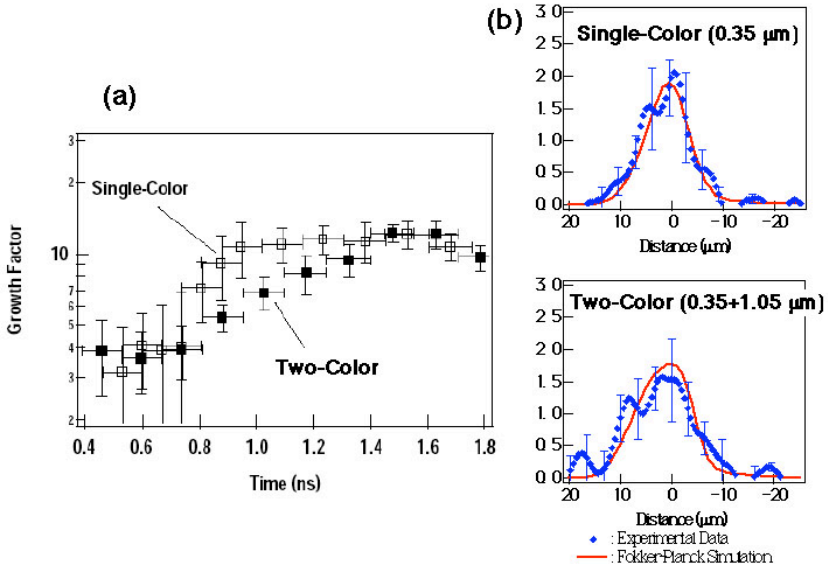

Fig. 4. (a) Rayleigh-Taylor growth factor for the one-color irradiation at 0.35-μm laser wavelength and for the two-color irradiation at 0.35- plus 0.53-μm wavelengths. (b) Density profiles for the generic one-color irradiation at 0.35-μm laser wavelength and the two-color irradiation at 0.35- plus 1.05-μm wavelengths. No significant degradation of the target density is seen.

substantial fraction of the temperature scale-length. The heated electrons are then nonlocally transported from the critical density region to the ablation region, deposit the energy, and modify the density profile there. This nonlocal effect may reduce the RT growth rate by enlarging the density scale-length and, in overkill case, reducing the ablation density. However, if the laser wavelength becomes 0.35 μm or shorter, that is suitable to obtain high ablation pressure necessary for high-density compression, the nonlocal effect becomes insignificant because of the higher critical density and the lower electron temperature associated with the shorter wavelength of the laser light. We have proposed two-color laser irradiation scheme: nonlocal effect is enhanced with a 0.53 or 1.05-μm laser, whereas high ablation pressure is generated with a 0.35-μm laser [19].

Figure 4 shows the comparison of the growth factor for the two-color irradiation case with that for the generic one-color irradiation case. A 25-μm thick polystyrene (CH) targets with initially imposed perturbation of 20-μm wavelength on the laser irradiation side were irradiated with 0.53-μm laser light overlapped to the 0.35- μm main drive laser light. The growth factor is defined as the areal mass perturbation divided by the initial perturbation. The RT growth saturates at around a growth factor of about 10, where the perturbation amplitude exceeds 1/10 of the perturbation wavelength. The gradient of the growth factor before the saturation is much smaller for the two-color case than that for the single color case.

As in any other schemes, the target should be well integrated. Figure 4 (b) shows the density profile of the generic one-color (0.35 μm) and two-color (0.35 plus 0.53 μm) irradiation measured with the penumbral imaging. Quite moderate density reduction and increase of the density scale-length are observed. The measured density profiles are in good agreement with the prediction by ILESTA-1D simulation with Fokker-Planck treatment for the nonlocal electron heat transport.

5. Impact Ignition

The sufficient suppression of the RT instability not only increases compressed density, but it may also revive an old ignition idea: High velocity implosion with 10^8 cm/s may configurate a hot-spark without a main fuel so as to ignite at very low laser energy of 30-100 kJ. This idea was rejected by two major criticisms: One, the RT instability limits the maximum implosion velocity well below the required velocity. Two, there is no pathway towards high gain. The first criticism may be overcome by introducing one of the new suppression schemes. The second criticism may be solved by impact ignition configuration recently proposed by Murakami et al. [34]. A main fuel is first imploded by laser, whereas the ignition is made by impact collision of the second partial shell with high velocity of 10^8 cm/s. There are several advantages in this idea:

1) This can be high-gain because a main fuel is introduced.
2) Simple because the main physics is hydrodynamics.
3) Low cost because no need of expensive pulse compressors.

A preliminary calculation by 2D hydrodynamic code PINOCO [35] shows that the high velocity part of the target is converted to high temperature and high density igniter surrounded by a low temperature high-density main fuel. This is the configuration that is desired for high-gain IFE targets.

6. Summary

We summarize the paper as follows. The strategy to test our understanding of the ablative Rayleigh-Taylor instability was to measure all necessary quantities (growth rate, gravity, mass flux across the unstable ablation surface, ablation density, and density

scale-length). The RT instability was found to be more stable than that the Takabe-Bodner formula with Betti's coefficient predicts. New schemes (double ablation and two color irradiation) are both attractive to adequately suppress the RT instability. RT suppression is the key element not only for higher density compression but for new impact ignition.

References

[1] R. Kodama et al., Nature 412 (2001) 798; ibid. 418 (2002) 933.
[2] H. Azechi et al., Laser and Part Beam 9 (1991) 193.
[3] H. Takabe et al., Phys. Plasmas 28 (1985) 3676.
[4] S. Bodner, Phys. Rev. Lett. 33 (1974) 761.
[5] R. Betti et al. Phys. Plasmas 5 (1998) 1446.
[6] H.J. Kull and S.I. Anisimov, Phys. Fluids 29 (1986) 2067.
[7] J. Sanz, Phys. Rev. Lett. 73 (1993) 2700.
[8] A.R. Piriz, Phys. Plasmas 8 (2001) 997.
[9] B.A. Remington et al., Phys. Rev. Lett. 67 (1991) 3259.
[10] K. Shigemori et al., Phys. Rev. Lett. 78 (1997) 250.
[11] H. Azechi et al., Phys. Plasmas 4 (1997) 4079.
[12] S.G. Glendinning, Phys. Rev. Lett. 78 (1997) 3318.
[13] C. J. Pawley et al., Phys. Plasmas 6 (1999) 565.
[14] J. P. Knauer et al., Phys. Plasmas 7 (2000) 338.
[15] T. Sakaiya et al., Phys. Rev. Lett. 88 (2002) 145003.
[16] J. Lindl and W.C. Mead, Phys. Rev. Lett. 34 (1975) 1273.
[17] P.W. McKenty et al., Phys. Plasmas 8 (2001) 2315.
[18] S. Bodner et al., Phys. Plasmas 7 (2000) 2298.
[19] K. Shigemori et al., Bull. Am. Phys. Soc. 46 (2001) 286.
[20] S. Fujioka et al., Phys. Rev. Lett. 92 (2004) 195001; S. Fujioka et al., Phys. Plasmas 11 (2004) 2814.
[21] Haan S et al Proc. Inertial Fusion Science and Applications 2003 (Illinois: American Nuclear Society) p. 55
[22] H. Azechi et al., Annu. Prog. Rept. 2000 in ILE Osaka Univ. 41 (2001).
[23] C. Yamanaka et al., IEEE J. quantum Electron. QE-17 (1981) 1639.
[24] H. Nakano et al., J. Appl. Phys. 73 (1993) 2122; N. Miyanaga et al. Proc. 15th International Conference on Plasma Physics and Controlled Nuclear Fusion Research, Seville, 1994 (IAEA, Vienna, 1996), Vol. 3, p. 153.
[25] S. Skupsky et al., J. Appl. Phys. 66 (1989) 3456.
[26] G. Miyaji, et al. Opt. Lett. 27 (2002) 725; N. Miyanaga, Rev. Laser Eng. 32 (2004) 241.
[27] M. Matsuoka et al., Rev. Sci. Instrum. 70 (1999) 637.
[28] J. Delettrez et al., Phys. Rev. A 36 (1987) 3926.
[29] K. Shigemori et al., Rev. Sci. Instrum. 69 (1998) 3942.
[30] H. Takabe et al., Phys. Fluids 31 (1988) 2884. Recently Fokker-Planck transport has been implemented in the ILESTA-1D code, some information of which is described in A. Sunahara et al., Phys, Rev. Lett. 91 (2003) 095003.
[31] S. Fujioka, Rev. Sci. Instrum. 73 (2002) 2588.
[32] Y. Tamari, in Proc. Inertial Fusion Science and Applications 2001 (Elesevier, New York, 2002), p. 874.
[33] N. Ohnishi et al., J. Quant. Spectrosc. Radiat. Transfer 71 (2001) 551.
[34] M. Murakami et al., submitted to Phys. Rev. Lett.
[35] H. Nagatomo et al., Plasma Physics 669 (2003) 253.